

# Fashion DNA: Merging Content and Sales Data for Recommendation and Article Mapping

Christian Bracher, Sebastian Heinz, Roland Vollgraf \*  
Zalando Research  
{christian.bracher, sebastian.heinz, roland.vollgraf}@zalando.de

## ABSTRACT

We present a method to determine *Fashion DNA*, coordinate vectors locating fashion items in an abstract space. Our approach is based on a deep neural network architecture that ingests curated article information such as tags and images, and is trained to predict sales for a large set of frequent customers. In the process, a dual space of customer style preferences naturally arises. Interpretation of the metric of these spaces is straightforward: The product of Fashion DNA and customer style vectors yields the forecast purchase likelihood for the customer-item pair, while the angle between Fashion DNA vectors is a measure of item similarity. Importantly, our models are able to generate unbiased purchase probabilities for fashion items based solely on article information, even in absence of sales data, thus circumventing the “cold-start problem” of collaborative recommendation approaches. Likewise, it generalizes easily and reliably to customers outside the training set. We experiment with Fashion DNA models based on visual and/or tag item data, evaluate their recommendation power, and discuss the resulting article similarities.

## CCS Concepts

•Information systems → Recommender systems; Content analysis and feature selection; •Human-centered computing → Collaborative filtering; •Computing methodologies → Neural networks;

## Keywords

Fashion data, neural networks, recommendations

## 1. INTRODUCTION

Compared to other commodities, fashion articles are tough to characterize: They are extremely varied in function and

\* postal address of all authors: Zalando SE, Charlottenstr. 4, 10969 Berlin, Germany

Permission to make digital or hard copies of part or all of this work for personal or classroom use is granted without fee provided that copies are not made or distributed for profit or commercial advantage and that copies bear this notice and the full citation on the first page. Copyrights for third-party components of this work must be honored. For all other uses, contact the owner/author(s).

KDD 2016 Fashion Workshop, August 14, 2016, San Francisco, CA, USA

© 2016 Copyright held by the owner/author(s).

ACM ISBN 978-1-4503-2138-9.

DOI: 10.1145/1235

appearance and lack standardization, and hence are described by a virtually open-ended set of properties and attributes, including labels such as brand (“Levi’s”) and silhouette (“jeans”), physical properties like shape (“slim cut”), color (“blue”), and material (“stonewashed cotton denim”), target groups (“adult,” “male”), price, imagery (photos, videos), and customer and expert sentiments. Many of these attributes are subjective or evolve over time; others are highly variable among customers, such as fit and style.

Zalando is Europe’s leading online fashion platform, operating in 15 countries, with a base of  $> 10^7$  customers and a catalog comprising  $> 10^6$  articles (SKUs), with  $> 10^5$  SKUs available for sale online at any given moment. Given the incomprehensibly large catalog and the heterogeneity of the customer base, matching shoppers and articles requires an automated pre-selection process that however has to be personalized to conform to the customers’ individual styles and preferences: The degree to which items are similar or complement each other is largely in the eye of the beholder. At the same time, proper planning at a complex organization like Zalando requires an “objective” description of each fashion item – one that is traditionally given by a curated set of labels like the above-mentioned. Still, these “expert labels” are often ambiguous, cannot consider the variety of opinion found among shoppers, and often do not even match the consensus amongst customers.

We set ourselves the task to find a mathematical representation of fashion items that permits a notion of similarity and distance based on the expert labels, as well as visual and other information, but that is designed to maximize sales by enabling tailored recommendations to individual clients. Our vehicle is a deep feedforward neural network that is trained to forecast the individual purchases of a sizable number ( $10^4 \dots 10^5$ ) of frequent Zalando customers, currently using expert labels and catalog images for  $\sim 10^6$  past and active Zalando articles as input. For each SKU we compute the activation of the topmost hidden layer in the network which we call its *Fashion DNA* (fDNA). The idiosyncratic style and taste of our shoppers is then simultaneously encoded as a vector of equal dimension in the weight matrix of the output layer. Inner products between vectors in these two dual spaces yield a likelihood of purchase and also express the similarity of fashion articles. Section 2 explains the mathematical model and presents the architecture of our network.

Collaborative-filtering based recommender systems [3, 1] suffer from the “cold-start problem” [10]: Individual predictions for new customers and articles cannot be calculated in

the absence of prior purchase data. Training of our network relies on sales records *and* content-based information on the article side, while only purchase data is used for customers. Once trained, the model computes fDNA vectors based on content article data alone, thus alleviating the “cold-start problem.” Our experiments show that the quality of such recommendations is only moderately affected by the lack of sales data. Likewise, it is easy to establish style vectors for unseen customers (by standard logistic regression), and their forecast performance is almost indistinguishable from training set customers. The generalization performance of our Fashion DNA model is demonstrated in Section 3.

As Fashion DNA combines item properties and customer sales behavior, distances in the fDNA space provide a natural measure of article similarity. In Section 4, we examine the traits shared by neighboring SKUs, and use dimensionality reduction to unveil a instructive, surprisingly intricate landscape of the fashion universe.

## 2. THE FASHION DNA MODEL

We now proceed to describe the design of the network that yields the Fashion DNA. It ingests images and/or attribute information about articles, and tries to predict their likelihood of purchase for a group of frequent customers. After training, item fDNA is extracted from the internal activation of the network.

### 2.1 Input data

For our experiments, we selected a “standard” SKU set of 1.33 million items that were offered for sale at Zalando in the range 2011–2016, mostly clothing, shoes, and accessories, but also cosmetics and housewares. For each of these articles, one JPEG image of size  $177 \times 256$  was available (some article images had to be resized to fit this format). Most of these images depict the article on a neutral white background; a few were photographed worn by a model.

We furthermore used up to six “expert labels” to describe each item. These tags were selected to represent distinct qualities of the article under consideration: Besides the brand and main color, they comprise the commodity group (encoding silhouette, gender, age, and function), pattern, and labels for the retail price and fabrics composition. Price labels were created using  $k$ -means clustering [4] of the logarithm of manufacturer suggested prices (MSRPs). For the fabrics composition labels, a linear space spanned by possible combinations of about 40 different fibers (e. g., cotton and wool) was segmented into 80 clusters. Labels were issued only where applicable; for instance, fabric clusters are restricted to textile items. Generally, only labels with a minimum number of 50 SKUs were retained. The number of different classes per label, and the percentage of articles tagged, are shown in Table 1. Label information was supplied to the network in the form of one-hot encoded vectors of combined length 3,855. Missing tags were replaced by zero vectors.

For validation purposes, the item set was randomly split 9:1 into a training subset  $\mathcal{I}_t$  of  $N_t \sim 1.2\text{m}$  and a validation subset  $\mathcal{I}_v$  of  $N_v \sim 130\text{k}$  articles.

### 2.2 Purchase matrix

The Fashion DNA model is trained and evaluated on purchase information which we supply in the form of a sparse boolean matrix  $\Pi$ , indicating the articles that have been

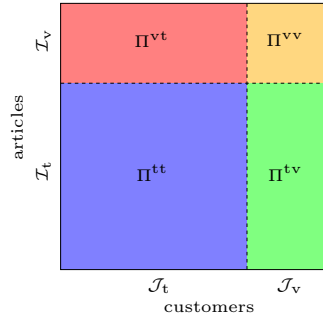


**Figure 1: Illustration of the purchase matrix  $\Pi$ . Every entry  $\Pi_{ij} \in \{0, 1\}$  encodes whether customer  $j$  has bought article  $i$ . Since we split the articles as well as the customers into a validation and a training set, the purchase matrix  $\Pi$  consists of four parts.**

bought by a group of 30,000 individuals that are among Zalando’s top customers. Their likelihood of purchase, averaged over all customer-SKU combinations, was  $p_{\text{avg}} = 1.14 \cdot 10^{-4}$ , amounting to 150 orders per customer in the standard SKU set. We task the network to forecast these purchases by assigning a likelihood for a “match” between article and customer.

As we are interested in the generalization of these predictions to the many Zalando customers not included in the selection, we likewise split the base of 30,000 customers 9:1 into a training set  $\mathcal{J}_t$  of  $K_t = 27,000$  customers and a validation set  $\mathcal{J}_v$  of  $K_v = 3,000$  customers, where care has been taken that the purchase frequency distributions in the two sets are aligned.

Hence, the purchase matrix is made of 4 parts, compare Figure 1:

training data	$\Pi^{tt} = (\Pi_{i,j})_{i \in \mathcal{I}_t, j \in \mathcal{J}_t}$ ,
SKU validation data	$\Pi^{vt} = (\Pi_{i,j})_{i \in \mathcal{I}_v, j \in \mathcal{J}_t}$ ,
customer validation data	$\Pi^{tv} = (\Pi_{i,j})_{i \in \mathcal{I}_t, j \in \mathcal{J}_v}$ ,
SKU-customer validation data	$\Pi^{vv} = (\Pi_{i,j})_{i \in \mathcal{I}_v, j \in \mathcal{J}_v}$ .

We are going to deal with each of these parts separately.

### 2.3 Mathematical model

A possible strategy to solve a recommender problem is by logistic factorization [7], [8] of the purchase matrix  $\Pi$ . Following that strategy, the probability  $p_{ij}$  is defined by

$$p_{ij} = P(\Pi_{ij} = 1) = \sigma(\mathbf{f}_i \cdot \mathbf{w}_j + b_j), \quad (1)$$

where  $\sigma(x) = [1 + \exp(-x)]^{-1}$  is the logistic function. Moreover,  $\mathbf{f}_i$  is a factor associated with SKU  $i$ ,  $\mathbf{w}_j$  a factor and  $b_j$  a scalar associated with customer  $j$ . During training, when

Tag Description	Class Count	Coverage
Brand code	2,401	97.2%
Commodity group	1,224	98.6%
Main color code	75	99.3%
Pattern code	47	32.6%
Price cluster	28	100.0%
Fabric cluster	80	64.9%

**Table 1: Article tags used for network training**

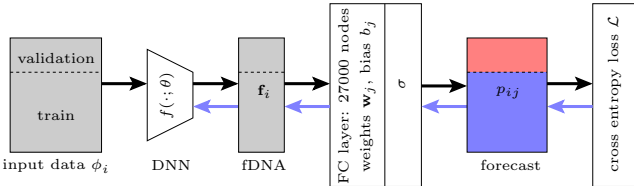


**Figure 2:** Schematic network architecture for Fashion DNA retrieval: training set customers. Article information (left) is passed through a deep neural network (DNN) to generate fDNA. The output is combined with customer-specific weights  $w_j$  and biases  $b_j$  in a fully connected layer and transformed into customer-item pair purchase probabilities by logistic regression (Eq. (1)). These forecasts are compared to the actual purchase matrix  $\Pi$  (ground truth) in a cross-entropy loss layer (Eq. (2)). The loss for the training set of articles is minimized by backpropagation (indicated by blue arrows).

we are dealing with the segment  $\Pi^{tt}$  of the purchase matrix, the quantities  $\mathbf{f}_i$ ,  $\mathbf{w}_j$  and  $b_j$  are adjusted such that the (mean) cross entropy loss

$$\mathcal{L}_{tt} = -\frac{1}{N_t K_t} \sum_{i \in \mathcal{I}_t} \sum_{j \in \mathcal{J}_t} [\Pi_{ij} \log p_{ij} + (1 - \Pi_{ij}) \log (1 - p_{ij})] \quad (2)$$

gets minimized. We define cross entropy losses on the remaining parts  $\Pi^{vt}$ ,  $\Pi^{tv}$  and  $\Pi^{vv}$  by changing the index sets in (2) appropriately.

Our method is based on Equations (1) and (2), yet, it yields a “conditioned factorization” only. Instead of learning the factor  $\mathbf{f}_i$  directly from the purchase data, we derive  $\mathbf{f}_i$  in a deterministic way via the SKU feature mapping

$$\mathbf{f}_i = f(\phi_i; \theta), \quad (3)$$

where  $\phi_i$  collects article features and metadata for SKU  $i$ . Moreover,  $f$  is a family of nonlinear functions given by a deep neural network (DNN), and  $\theta$  are parameters which are learned by our model. We remark that “deep structured semantic models” [5] solve problems similar to the one studied here.

For every article  $i$  let us identify  $\mathbf{f}_i$  as its fDNA. Likewise, we can think of  $\mathbf{w}_j$  as the “style DNA” reflecting the individual preferences of customer  $j$ . The bias  $b_j$  is a measure for the overall propensity of customer  $j$  to buy.

In addition to training, there are three validation procedures:

1. **Training:** The purchase data in  $\Pi^{tt}$  is used to train the network parameters  $\theta$  and the customer weights  $\mathbf{w}_j$  and biases  $b_j$ ,  $j \in \mathcal{J}_t$ , in order to perform the logistic matrix “conditioned factorization” via (1), as sketched in Figure 2. The loss is given by Equation (2).
2. **SKU validation:** For SKUs not seen during training,  $\Pi^{vt}$  contains purchases of the training customers. Validation is straightforward: Part 1 yields the weights  $\mathbf{w}_j$  and bias  $b_j$  for a training customer  $j \in \mathcal{J}_t$ , as well as the parameters  $\theta$ . We then compute the fDNA  $\mathbf{f}_i$  for SKUs  $i \in \mathcal{J}_v$  via Equation (3).

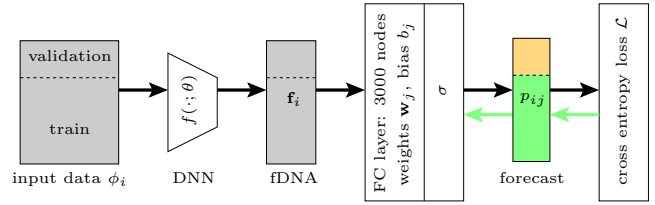


**Figure 3:** Schematic network architecture for Fashion DNA retrieval: validation set customers. For a hold-out set of customers, backprop (green arrows) is limited to the weights and biases, leaving the fDNA fixed. Evaluation of performance mainly takes place on the combined validation set of customers (orange).

3. **Customer validation:** Validation of new customers only works indirectly. It requires additional training of parameters, i. e., we have to find weights  $\mathbf{w}_j$  and biases  $b_j$  for the new customers  $j \in \mathcal{J}_v$ . This amounts to  $K_v$  simultaneous logistic regression problems from  $\mathbf{f}_i$  to  $\Pi_{ij}$ , where the  $\mathbf{f}_i$  are taken from Part 1 (see Figure 3). The validation loss  $\mathcal{L}_{tv}$  measures the fDNA’s ability to linearly predict purchase behavior for such customers. High values compared to the training loss  $\mathcal{L}_{tt}$  indicate that the SKU feature mapping  $f(\cdot; \theta)$  does not generalize well to validation set customers.

4. **SKU-customer validation:** Eventually, on  $\Pi^{vv}$ , we measure whether the logistic regression learned during customer validation in Part 3 generalizes well to unseen SKUs, analogous to the procedure in Part 2. The factors  $\mathbf{w}_j$  now correspond to the validation customers  $j \in \mathcal{J}_v$ , which were derived in Part 3 by means of logistic regression.

## 2.4 Neural network architecture

We experimented with three different multi-layer neural network models (DNNs) that transform attribute and/or visual item information into fDNA. The width of their output layers defines the dimension  $d$  of the Fashion DNA space (in our case,  $d = 256$ ). This fDNA then enters the logistic regression layer (Figures 2 and 3).

### 2.4.1 Attribute-based model

Here, we used only the six attributes listed in Table 1 as input data. As described in Section 2.1, these “expert” tags were combined into a sparse one-hot encoded vector that was supplied to a four-layer, fully connected deep neural network with steadily diminishing layer size. Activation was rendered nonlinear by standard ReLUs, and we used drop-out to address overfitting. The output yields “attribute Fashion DNA” based only on the six tags.

### 2.4.2 Image-based model

This model is based purely on visual data, and feeds Zalando catalog images (see Section 2.1 for details) into an eight-layer convolutional neural network based on the AlexNet architecture [9], resulting in “image fDNA.”.

### 2.4.3 Combined model

Finally, we integrated the attribute- and image-based architectures into a combined model. We first trained both

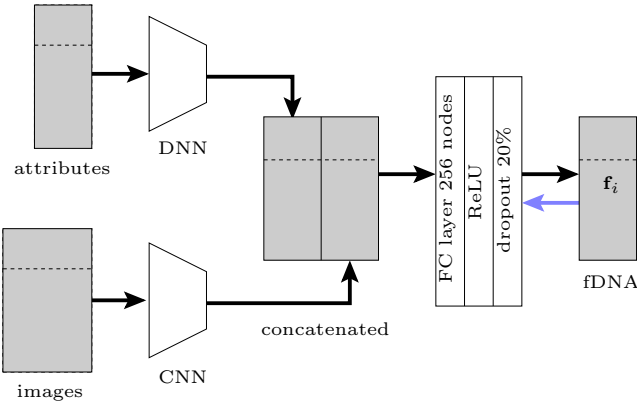


**Figure 4:** Combining attribute- and image-based Fashion DNA. Article data flow through the respective pre-trained networks (see Sections 2.4.1 and 2.4.2); the resulting attribute and image fDNAs are concatenated to a vector of dimension  $2d$  which is subsequently halved in size by a fully connected layer with ReLU nonlinearity. Only the weights in the merging layer are adjusted by backpropagation from the logistic regression layer in Figures 2 and 3.

networks and then froze their weights, so their outputs are the fDNA in either model. The outputs are concatenated into a single input vector, then supplied to a fully connected layer with adjustable weights that condenses this vector into the fDNA vector of the model. This layer, together with the logistic regressor, was trained by backpropagation as described above. The architecture is sketched in Figure 4.

All three models were implemented in the Caffe framework [6] and used to generate fDNA vectors for the standard SKU set, with corresponding customer weights and biases. For training, the weights of the logistic regression layer are initialized with Gaussian noise, while the bias is adjusted to reflect the individual purchase rate of customers on the training SKU set. The resulting fDNA vectors are sparse (about 30% non-zero components), leading to a compact representation of articles.

### 3. FDNA-BASED RECOMMENDATIONS

A key objective of Fashion DNA is to match articles with prospective buyers. Recall that the network yields a sale probability  $p_{ij}$  for every pair of article  $i$  and customer  $j$ ; it is therefore natural to rank the probabilities by SKU for a given customer to provide a personalized recommendation, or to order them by customer to find likely prospective buyers for a fashion item. In this section, we examine the properties of fDNA-based item recommendations for customers.

#### 3.1 Probability distribution

Predicted probabilities span a surprisingly large range: The least likely customer–item matches are assigned probabilities  $p_{ij} < 10^{-12}$ , too low to confirm empirically, while the classifier can be extraordinarily confident for likely pairings, with  $p_{ij}$  approaching 50%.

To be valuable, quantitative recommendations need to be *unbiased*: The predicted probability  $p_{ij}$  should accurately reflect the observed chance of sale of the item to the customer. As sales are binary events, comparing the probability

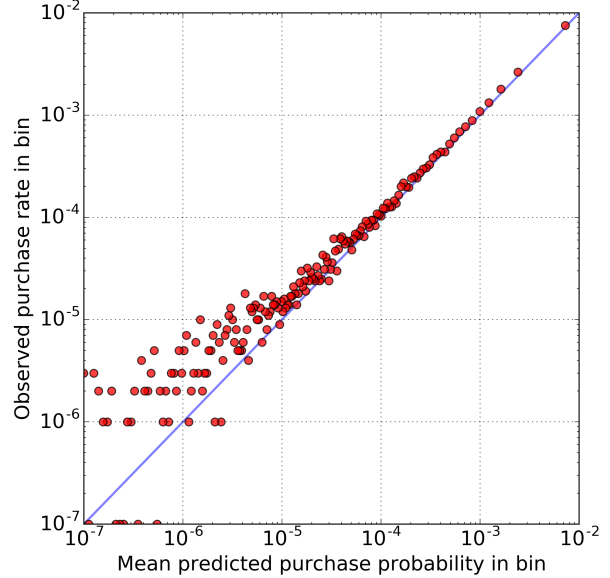


**Figure 5:** Predicted probability vs. actual purchase rate for pairs in the customer–item validation set ( $\Pi^{VV}$ ) for the combined attribute–image network model. Each point represents a bin of  $10^6$  pairs with similar predicted probability, taken from a random sample of  $2 \cdot 10^8$  pairs. Bins with average probabilities  $< 10^{-7}$  (representing  $\sim \frac{1}{8}$  of the sample) are not shown.

with the ground truth requires aggregating many customer–article pairs with similar predicted likelihoods in order to evaluate the accuracy of the forecast. As the average likelihood of an article–customer match is small (on the order of only  $10^{-4}$  even for the frequent shoppers included here), comparisons are affected by statistical noise, unless large sample sizes are used. Fortunately, our model yields about  $4 \cdot 10^9$  combinations of customers and fashion items in the respective validation sets.

An analysis of this type reveals that our models indeed are largely devoid of such bias, as Figure 5 illustrates. For the analysis,  $2 \cdot 10^8$  customer–item pairs have been sampled in the validation space, and then sorted into 200 bins by probability. In the figure, the average probability of the  $10^6$  members of each bin is compared to the number of actual purchases per pair. The predicted and empirical rates track each other closely, save for pairs considered very unlikely matches by the regressor. In this regime, the model underestimates the empirical purchase rate which settles to a base value of about  $1.5 \cdot 10^{-6}$ .

#### 3.2 Recommendation quality

In some contexts, quantitative knowledge of the predicted purchase likelihood is less relevant than ranking a set of fashion articles by the preference of individual customers. The overall quality of such a ranking can be illustrated by receiver operating characteristic (ROC) analysis.

##### 3.2.1 ROC analysis

An ideal model would rank those SKUs in the hold-out

AUC Score	Training SKUs		Validation SKUs	
	$\Pi^{tt}$	$\Pi^{tv}$	$\Pi^{vt}$	$\Pi^{vv}$
by attribute	0.944	0.940	0.915	0.916
by image	0.941	0.937	0.877	0.877
combined	<b>0.967</b>	<b>0.963</b>	<b>0.933</b>	<b>0.932</b>

**Table 2: AUC scores by network model**

set highest that were actually bought by the customer. In reality, of course, the model will give preference to some items not chosen by the customer, and the number of “hits” and “misses” will both grow with the number of recommendations issued, or, equivalently, with a decreasing purchase probability threshold. A common technique to analyze the performance of such a binary classifier with variable threshold is ROC analysis [4]. The ROC diagram displays the number of recommended sold items (the “hits,” or in the parlance of ROC, the “true positives”), as a function of recommended, but not purchased items (the “misses,” or “false positives”). As the threshold probability is reduced from 1 to 0, the true and false positive rates trace out a ROC curve leading from the lower left to the upper right corner of the diagram. As overall higher true positive rates indicate a more discriminating recommender, the area under the ROC curve (AUC score) is a simple indicator of the relative performance of the underlying model [2], with  $AUC = 1.0$  being ideal, whereas  $AUC = 0.5$  is no better than guessing (diagonal line in diagram).

In principle, ROC analysis yields an individual curve and AUC score for each customer  $j$ , and will depend on the choice of fDNA model. To evaluate generalization performance, we aggregated numerous customer-article pairs ( $2 \cdot 10^8$ ) for each of the four training/validation combinations  $\Pi^{tt}$ ,  $\Pi^{vt}$ ,  $\Pi^{tv}$ ,  $\Pi^{vv}$ , predicted purchase likelihood, and conducted a “synthetic” ROC analysis on this data that presents an average over many customers instead. We repeated this calculation for each fDNA model. The outcomes are listed in condensed form as average AUC scores in Table 2.

### 3.2.2 Generalization performance

Before we discuss model performance in detail, we examine to which extent information gleaned from the training of our models is transferable to fashion items (e.g., SKUs newly added to the catalog) and customers outside the training set.

Table 2 tells us that for a given fDNA model, the AUC score is highest if both customers and articles are taken from the training sets ( $\Pi^{tt}$ ), diminishes as one of the groups is switched to the validation set ( $\Pi^{vt}$ ,  $\Pi^{tv}$ ), and becomes lowest when both customers and articles are taken from the hold-out sets ( $\Pi^{vv}$ ), as expected. But the scores conspicuously pair up: For a given SKU set (training or validation), there is very little difference in AUC score between the training and validation set customers. This observation holds irrespective of the specific fDNA model employed.

Picking the most powerful fDNA model based on images and attributes, we determined ROC curves for the four cases laid out in Figure 1. Adopt the color code defined there, we display the curves in Figure 6. Indeed, the ROC curves for  $\Pi^{tt}$  (blue) and  $\Pi^{tv}$  (green) track each other closely, as do the curves for validation set articles  $\Pi^{vt}$  (red) and  $\Pi^{vv}$  (orange). We conclude that our approach generalizes extremely well to hold-out customers, at least when they shop at a similar

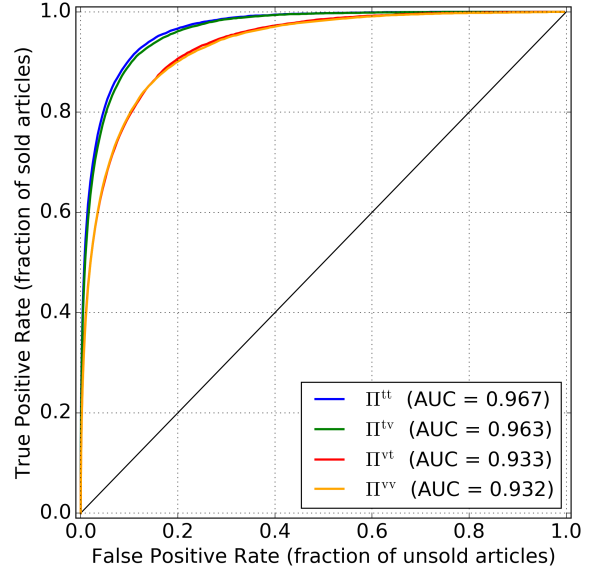


**Figure 6: Comparison of recommendation performance for training and validation set items and customers in the combined attribute–image fDNA model. The ROC curves for validation set customers (green, orange) closely follow the corresponding curves for training set customers (blue, red). There is a more pronounced difference between training set SKUs (blue, green) and hold-out SKUs (red, orange). Color scheme as in Figure 1.**

rate.

Next, we address another related aspect of generalization performance for our model architecture: How well does recommendation quality in the article training set correlate with the quality for items in the hold-out set for a given customer? Recommendation theory sometimes posits that most customers fall in well-defined groups that have aligned preferences, except for a few “black sheep” with idiosyncratic behavior that cannot be forecast well. However, given the extreme amount of choice, and the sparsity of sales coverage, it can be argued that idiosyncrasy in fashion taste and style is the norm rather than the exception.

To investigate, we compiled recommendations for a large group of individual customers for both article training and validation sets, and compared them to their actual purchases in both sets. Then, we examined the resulting pairs of customer-specific AUC scores for correlation. Figure 7 displays a scatterplot of such scores for the combined attribute–image fDNA model, using the hold-out customer set. Although regression analysis reveals a weak dependency (Pearson coefficient of correlation  $R^2 \approx 0.09$ ), the plot is dominated by random statistical fluctuation, likely caused by the small number of sales events for any given customer. There is little evidence for “black sheep” with consistently low AUC scores, nor are there visible clusters.

### 3.2.3 Model comparison

While switching from training to validation set customers

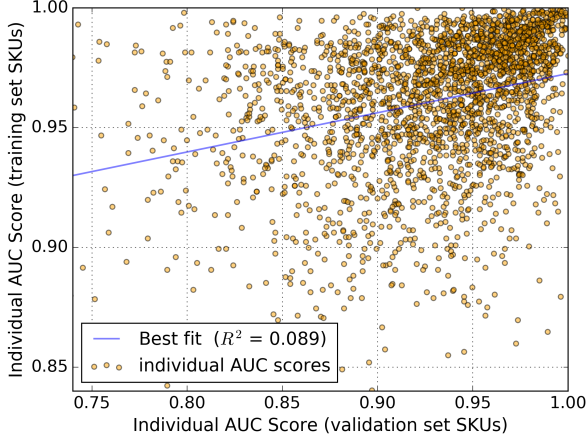


**Figure 7: Individual AUC scores in the combined fDNA model.** The plot compares recommendation performance for training and validation set SKUs for 3,000 customers in the hold-out set. Correlation of scores between the two sets is weak.

hardly affects recommendation performance, there is a clear difference between the three fDNA models introduced in Section 2.4 when the generalization to validation set articles is examined instead (Table 2). Although attribute- and image-based fDNA perform at nearly equal levels in the training SKU set, the image-based model is distinctly inferior for articles in the validation set. Although this observation suggests that mere visual similarity is a worse predictor for customer interest than matching attributes, it might also involuntarily result from the widespread use of article attributes in search filters and recommendation algorithms that prejudice choice when customers browse the online shop.

As we are particularly interested in the ability of the models to generalize to unseen items and validation set customers, we calculated ROC curves from the probability forecasts for the segment  $\Pi^{VV}$  (orange sector in Figure 1). They are shown in Figure 8. The plot reveals that a ranking based on only six attributes (dashed curve) beats recommendations based on the much richer image fDNA (dotted curve). As possible causes behind this observation, we note that items with very different function may look strikingly similar (e. g., earmuffs and headphones), and that minor details may alter the association of an article with a customer group (for instance, men’s and women’s sport shoes often look much alike). As mentioned, users commonly select attributes as filter settings for the Zalando online catalog, so the better performance of attribute fDNA may also reflect the shopping habits of our customers. Importantly, we point out that integrating attribute and image information boosts recommendation performance considerably, as the ROC curve for the combined model fDNA (solid curve) shows. This indicates that images and attributes carry complementary information.

For a more practical interpretation of the ROC analysis, we turn to Figure 9, which provides a magnified view of the ROC curves near the origin, i.e., for small true and false positive rates. We note that the “positive” (articles purchased) and “negatives” classes in this case are extremely unbalanced

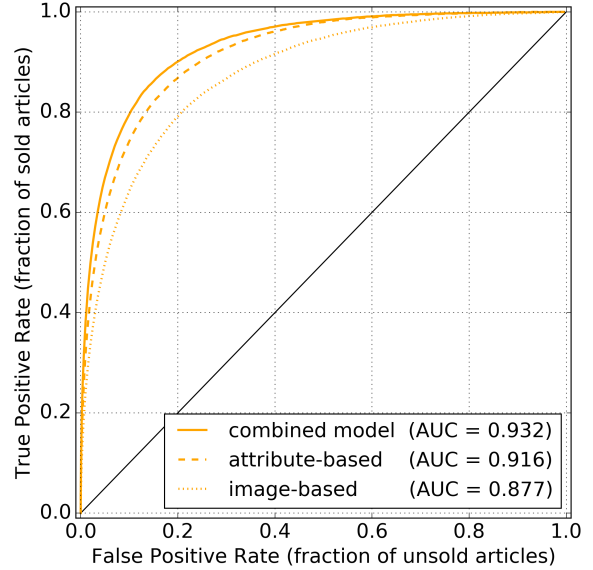


**Figure 8: Recommendation strength of different Fashion DNA models, evaluated for SKU–customer validation data  $\Pi^{VV}$  (orange sector in Figure 1).** The attribute-based model (dashed curve) outperforms image-based fDNA (dotted curve). Combining attributes and images yields a superior fDNA model (solid line). The black diagonal line represents random guess performance.

(the average customer only acquires 0.01% of the article set). Hence, to a very good approximation, all 120k articles in the validation set are negatives, and the rate of false positives shown on the abscissa is essentially equivalent to the ratio of the number of recommended articles to the validation set size. (For instance, a false positive rate of  $10^{-4}$  represents the top-12 recommended articles.) From the figure, we infer that the top recommendation represents about 0.8% of validation set purchases in the combined fDNA model — for the average validation customer buying 17 items in the validation SKU set, this translates to a 13% “success rate” of the recommendation. For top-12 (top-120) recommendation, one captures 3.5% (13%) of the items bought by shoppers similar to the ones in the customer training set. (Of course, this ex-post-facto analysis cannot predict to which extent a customer would have bought the top-rated items, had they been suggested to her as recommendations. This question properly belongs to the domain of A/B testing.)

### 3.3 A Case Study

For illustration, we now present the leading recommendations of validation set articles for a sample frequent customer, a member of the training set, and compare results from the three Fashion DNA models introduced earlier. (For lack of space, we only discuss a single case here. Our observations hold quite generally, though.)

Figure 10 displays the top-20 recommended fashion items for the attribute-based model (top row), image-based model (second from top), and the combination model, our strongest

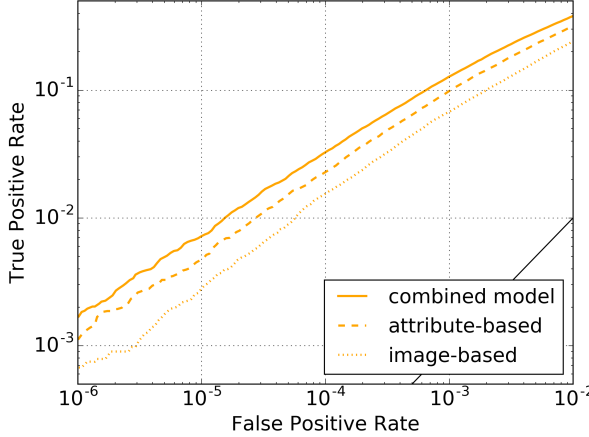


**Figure 9: Recommendation performance in the small sample size limit. The logarithmic ROC plot is a detailed view of the lower left corner in Figure 8.**

contender (third row). The estimated likelihood of purchase decreases from left to right, with the first choice exceeding 10%; the mean forecast probability of sale for the articles on display hovers around 5%. For contrast, we also display the items deemed *least* likely in the combination model (fourth row). There, the model estimates a negligible chance of sale (around  $10^{-8}$ %). Actual consumer purchases are on view in the bottom rows.

Note that the items suggested by attribute fDNA, due to the lack of visual information in training, appear quite heterogeneous. The underlying similarity, typically matching brands, remains concealed in the image. (Among the attributes in Table 1, the brand and commodity group tags claim the lion’s share of information, and major brands commonly try to gain market share by covering the whole fashion universe, from shoes to accessories.) Although quite successful for our sample customer (one item highlighted in green was bought, and the top-100 recommendations capture four sales), the selection does not reflect her predilection with red and pink hues. Unsurprisingly, image-based fDNA yields a visually more uniform result, often aggregating items with a very similar look, here striped and pink shirts. Although pleasing to the eye, the approach is less successful. (None of the items shown was acquired, and there was a single “hit” in the top 100 suggestions.) The combination model integrates the hidden features from the attribute model, and the visual trends (note that recommended SKUs from both models are taken over), and offers a compact, yet more varied selection. In line with the general observation, it is also the most performant model in our case study, with one item shown bought, and five within the top 100 selection. We finally remark that the least favorable items (bottom row) are by themselves a coherent group (boys’ clothes) that summarizes qualities this customer is *not* interested in: kids’ and men’s apparel, plaid patterns. This suggests that the models’ negative recommendations may be actionable as well.

## 4. EXPLORING ARTICLE SIMILARITY

As laid out in Section 2, a central tenet of our approach is the assignment of articles  $i$  to vectors  $\mathbf{f}_i$  in a Fashion

DNA space. Any metric in this space naturally defines a distance measure  $D_{ik}$  between pairs of fashion items. Cosine similarity is a simple choice that works well in practice:

$$D_{ik} = 1 - \frac{\mathbf{f}_i \cdot \mathbf{f}_k}{\sqrt{|\mathbf{f}_i|^2 |\mathbf{f}_k|^2}}. \quad (4)$$

Every fDNA model gives rise to its own geometrical structure that emphasizes different aspects of similarity.

### 4.1 Next Neighbor Items

We start out exploring local neighborhoods in the fDNA spaces. Picking a sample article (here, a maternity dress and a bow tie), we determine their angular distances (4) to the standard SKUs, and select the nearest neighbors according to the three fDNA models.. They are displayed in Figure 11.

For both SKUs, attribute-based fDNA yields a heterogeneous mixture of articles that hides the underlying abstract similarity: The nearest neighbors to the dress all share the same brand, and in the case of the bow tie, men’s accessories offered by various luxury brands are found. For the image-based fDNA, visual similarity is paramount; the search identifies many dresses aligned in color and style, photographed in a similar fashion. The same analysis for the bow tie reveals the risks underlying the visual strategy: Here, the algorithm picks completely unrelated objects that superficially look similar, like bras and a dog pendant. In either case, the most sensible results are returned by the combined attribute–image approach. For the dress, the nearby items are generally maternity attire that matches the original brand (note that the mismatched objects in the attribute-based selection are now filtered out). In the case of the bow tie, regular ties are identified as nearest neighbors: The algorithm has learned that ties and bow ties share the same role in fashion. We also point out that the combined fDNA has included a baby romper (of the same brand) in the neighborhood of the maternity dress – a clear sign that information propagates backward from the customer–item sales matrix into the fDNA model. Such conclusions are also inescapable when the global distribution of items in the fDNA space is studied.

### 4.2 Large-Scale Structure

While the number of fashion items offered by Zalando is huge from a human perspective, they occupy the 256-dimensional fDNA space only sparsely. In order to visualize the arrangement of SKUs on a larger scale, we resort to dimensionality reduction techniques, and find that t-SNE (stochastic neighborhood embedding) is a suitable tool [11] to reveal the structure hidden in the data. The resulting maps are rather fascinating descriptions of a fashion landscape that combines hierarchical order at several levels with smooth transitions.

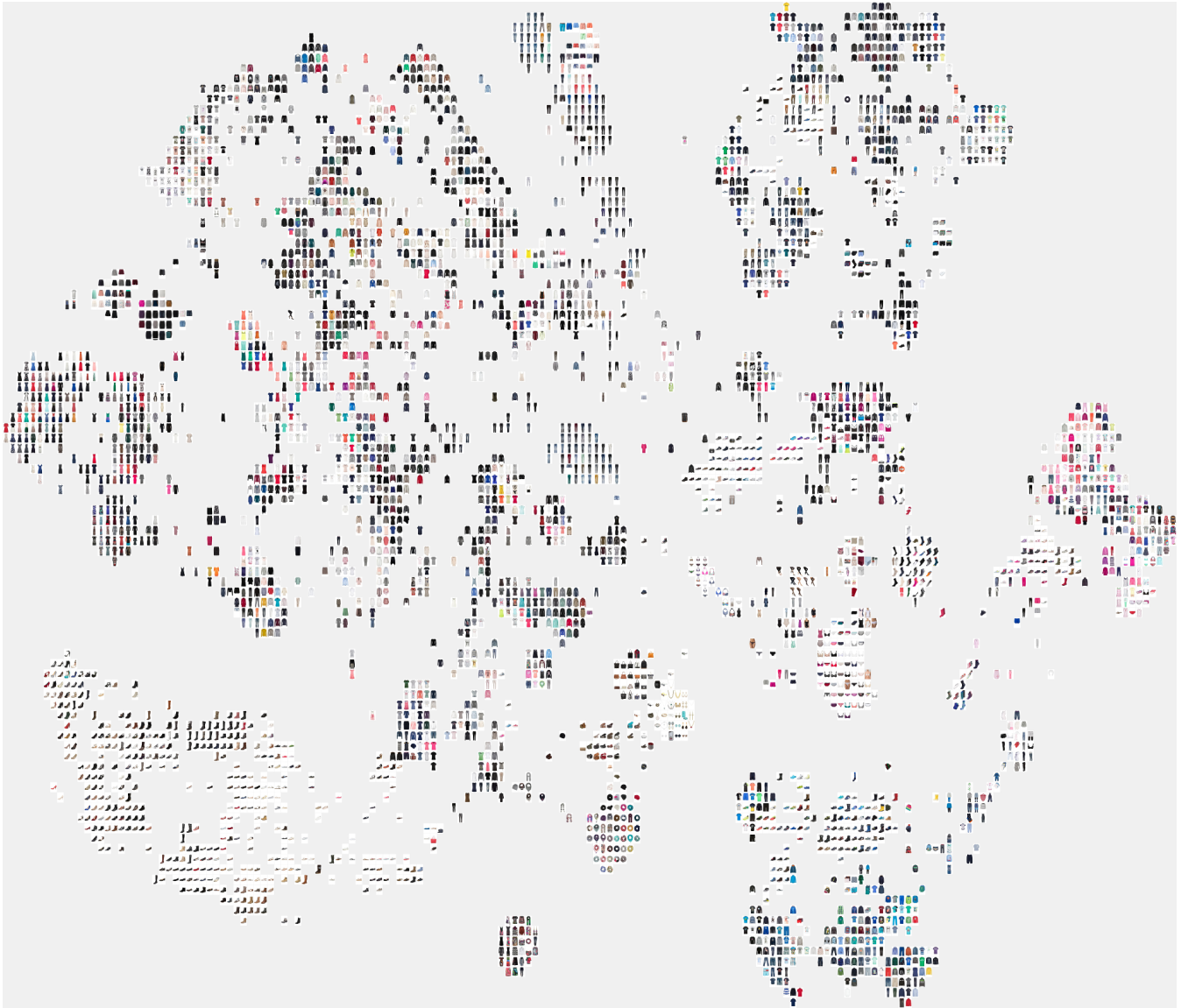
Figure 12 displays such a map, generated from 4,096 randomly drawn articles from the catalog (subject to the weak restriction that the articles be sold at least 10 times to our 100,000 most frequent customers). As underlying model, we used the combined attribute–image fDNA. A glance at the map already shows the presence of orderly clusters, but much interesting detail is revealed only when studying the arrangement in close-up view. (A high-resolution image of the t-SNE map is posted online.) In Figure 13, we provide a guide to some “landmarks” we found examining the image.



Figure 10: Validation set recommendations for a frequent customer. Top: Leading 20 recommendations from attribute-based fDNA (first row), image-based fDNA (second row), and combined fDNA (third row). The fourth row displays items judged least likely to be purchased in the combined model. Actual consumer purchases are displayed in the row pair at the bottom. Two matches are highlighted in green.



Figure 11: Next-neighbor items in the 1.33m article catalog. The two panels show next neighbors to the source items (maternity dress, bow tie) in the extreme left column, with cosine similarity decreasing to the right. Top rows: Attribute-based fDNA, center rows: image-based fDNA, bottom rows: combined model.



**Figure 12:** t-SNE map of 4,096 fashion articles picked at random from the catalog, using the combined fDNA model. Zoomable high-resolution view available online at <https://github.com/cbracher69/fashion-tsne-map>.

On the largest scale, the map is divided into three “continents”: On the upper right, men’s fashion items are assembled (**A**). The structure to the lower right contains kids’ apparel and shoes, neatly separated into boys’ (**B**) and girls’ fashion (**C**), connected by a narrow isthmus of baby (**D**) and maternity items (**E**). The huge remainder of the map (**F**) is devoted to women’s fashion gear, with a core body of assorted clothing (upper left), surrounded by satellites of casual and fashion shoes (**G**, lower left), accessories (**H**), lingerie, hosiery, and swimwear (**I**), and sport shoes and gear (**J**). Each of the regions is further subdivided (e. g., accessories (**H**) are separated into scarves (red), belts (green), hats (brown), bags (blue), jewelry (purple), and sunglasses (cyan)). It is remarkable that the separation at the top level is essentially complete, as there is for instance no mixing between male and female items. Instead, subcategories are replicated in each section (such as a male sports cluster (**K**))

that, naturally enough, faces the much larger female counterpart (**J**)). But there is also gradual progression in some structures: For instance, heel heights increase as one travels clockwise along the outer rim of the shoe cluster (with high heels (**L**) being opposite dresses (**M**) on the apparel side). Another example is kids’ clothing, where size and age group increases as one travels away from the maternity “center” (**E**). It is notable that at the lower levels of organization, clustering mostly occurs by shape or pattern, and only rarely by function (e. g., there is a “soccer cluster” (**N**) in the boys’ section), or brand loyalty, the *Desigual* “island” (**O**) at the very bottom being the only conspicuous example.

## 5. CONCLUSIONS

In this paper, we introduced the concept of Fashion DNA, a mapping of fashion articles to vectors using deep neural networks that is optimized to forecast purchases across a

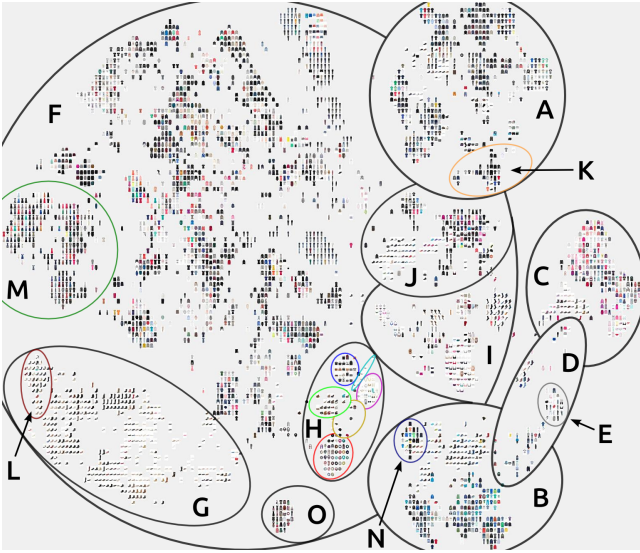


**Figure 13: A guide to highlights in the t-SNE fashion landscape.**

large group of customers. Being based on item properties, our approach is able to circumvent the cold start problem and provide article recommendations even in the absence of prior purchase records. Likewise, the model is flexible enough to generate sales probability predictions of comparable quality for validation customers. We demonstrated that an fDNA model based on article attributes and images generalizes well and suggests relevant items to shoppers. The combination of article and sales information imprints a wealth of structure onto the item distribution in fDNA space.

We plan to enrich the model with additional types of fashion-related data, such as ratings, reviews, sentiment, and social media, which will require extensions of the deep network handling the information, e. g. natural language processing capability. With an increasing number of information channels, for many items only partial data will be available. To render the network resilient to missing information, we will further experiment with drop-out layers in our architectures.

An important aspect currently absent in our model is the temporal order of sales events. Customer interest and item relevance evolve over time, whether by season, by fashion trends, or by personal circumstances. Capturing and forecasting such variations is a difficult task, but also a valuable business proposition that may be tackled by introducing long short-term memory (LSTM) elements into our network.

## 6. ACKNOWLEDGMENTS

We would like to thank Urs Bergmann for valuable comments on this paper.

## 7. REFERENCES

- [1] R. Bell, Y. Koren, and C. Volinsky. Modeling relationships at multiple scales to improve accuracy of large recommender systems. In *Proceedings of the 13th ACM SIGKDD International Conference on Knowledge Discovery and Data Mining*, KDD ’07, pages 95–104, New York, NY, USA, 2007. ACM.
- [2] P. Flach, J. Hernández-Orallo, and C. Ferri. A coherent interpretation of AUC as a measure of aggregated classification performance. In *Proceedings of the 28<sup>th</sup> International Conference on Machine Learning (ICML-11)*, pages 657–664, 2011.
- [3] D. Goldberg, D. Nichols, B. M. Oki, and D. Terry. Using collaborative filtering to weave an information tapestry. *Communications of the ACM*, 35(12):61–70, 1992.
- [4] T. Hastie, R. Tibshirani, and J. H. Friedman. *The Elements of Statistical Learning: Data Mining, Inference, and Prediction* (2nd ed.). Springer, New York, 2009.
- [5] P.-S. Huang, X. He, J. Gao, L. Deng, A. Acero, and L. Heck. Learning deep structured semantic models for web search using clickthrough data. In *Proceedings of the 22nd ACM International Conference on Information and Knowledge Management (CIKM)*, pages 2333–2338, 2013.
- [6] Y. Jia, E. Shelhamer, J. Donahue, S. Karayev, J. Long, R. Girshick, S. Guadarrama, and T. Darrell. Caffe: Convolutional architecture for fast feature embedding. *arXiv preprint arXiv:1408.5093*, 2014.
- [7] C. Johnson. Logistic matrix factorization for implicit feedback data. In *NIPS Workshop on Distributed Matrix Computations*, 2014.
- [8] Y. Koren, R. Bell, and C. Volinsky. Matrix factorization techniques for recommender systems. *IEEE Computer*, pages 42–49, 2009.
- [9] A. Krizhevsky, I. Sutskever, and G. E. Hinton. Imagenet classification with deep convolutional neural networks. In *Advances in neural information processing systems*, pages 1097–1105, 2012.
- [10] A. I. Schein, A. Popescul, L. H. Ungar, and D. M. Pennock. Methods and metrics for cold-start recommendations. In *Proceedings of the 25th annual international ACM SIGIR conference on Research and development in information retrieval*, pages 253–260, 2002.
- [11] L. van der Maaten and G. Hinton. Visualizing data using t-SNE. *Journal of Machine Learning Research*, pages 2579–2605, 2008.